Predictive-Equivalent Consumption Minimization Strategy for Energy Management of A Parallel Hybrid Vehicle for Optimal Recuperation

Emre KURAL*, Bilin Aksun GÜVENÇ**
* AVL GmbH, GRAZ, Austria
** Ohio State University, Columbus, USA.
(Geliş / Received : 10.10.2014 ; Kabul / Accepted : 12.11.2014)

ABSTRACT

The possibility to distribute the traction power in Hybrid Electric Vehicles powertrain over different prime movers and energy recoverability via recuperative braking as well as buffering the energy on rechargeable batteries, lead to the question of how electrical, mechanical or chemical energy should flow among various hybrid components of the powertrain. This optimization problem, mostly called energy management of hybrid electric vehicles aims to find the minimum consumed fuel energy flow, in other words fuel consumption over the entire trip. This study describes the application of theoretical global optimization method called Dynamic Programming (DP) and a practical approach substitute, namely Equivalent Consumption Minimization Strategy (ECMS) to a parallel hybrid powertrain energy management problem and their virtual tests in various drive-cycles. The computational burden of DP has been relaxed by ECMS approach and sub-optimal behaviour is rather comparable to global optimal behaviour. Finally, ECMS is enhanced by novel method based on predictive information to anticipate upcoming road topology in order to fully benefit either the free recuperation energy over long downhill road sections or via pre-charging strategy against uphill road sections.

Keywords: Hybrid electric vehicle energy management, Vehicle and powertrain modelling, optimization, predictive energy management

Paralel Hibrit Elektrikli Aracın, Optimal Reküperatif Frenleme için Öngörülü- Eşdeğer Yakit Tüketimi Minimizasyonu Startejisi ile Enerji Yöntemi

ÖZ

The cost of routing vehicles represents an important component of many transportation and distribution costs in a logistics system. The typical vehicle routing problem involves in designing a set of minimumcost routes for a fleet of vehicle. The vehicle routing problem with time windows is a generalization of the vehicle routing problem where the service of a customer can begin within the time window defined by the earliest and the latest times when the customer will permit the start of service.

In this study, The Vehicle Routing problem that root of the logistic systems is handled as Time Window Vehicle Routing Problem to obtain the routes of the vehicles that are used by the Arçelik Authorized Service. These vehicles distribute the products which were sold to Sincan and Etimesgut Regions in Ankara. Recommended model was structured and solved with real datas using Mix Integer Programming. With respect to the results the improvings are shown and the optimal routes are obtained. By the matematical model, the customers' demands, that authorized service provided with 761.399 km, could be also provided. The situation which the total distance could be reduced as 67.90% was demonstrated. The routes which could be provided on time and costed minimum was revealed.

Keywords: Logistic Systems, Vehicle Routing Problem, Vehicle Routing Problem with Time Windows

1. INTRODUCTION (GİRİŞ)

Legislative limits for pollutant exhaust emissions, CO_2 targets and increasing market demand for higher fuel economy in passenger cars motivate automotive industry to develop alternative powertrain such as Hybrid Electric Vehicle (HEV) and their innovative control technologies [1]. Today, many studies indicate the available diversity of these cars on the market which is a positive sign of rapidly increasing electro-mobility trends and their quick market penetration [2]. Moreover, economical potential of HEV and Plug-in-HEV for end-users is already demonstrated by many studies for their tremendous benefit in terms of greenhouse gas reduction and improved efficiency [3].

HEVs essentially store two different energy sources on board: electrical energy in battery and chemical energy in fuel tank. The traction power is obtained from these energy sources in powertrain consisting of combustion engine and electrical motors which is also able to recover electrically the braking energy via recuperative braking. Having these various back and forth energy

* *Sorumlu Yazar (Corresponding Author)*
e-posta:emrekural@gmail.com
Digital Object Identifier (DOI) : 10.2339/2015.18.3, 113-124

flow, necessitates an optimal distribution and management of energy flows in HEV powertrain.

This optimization of energy management has been addressed by many studies in literature and various methods have been proposed to find the optimal behaviour of the energy flows [4-5]. As a benchmark method, having the complete topology and speed profile of a driving scenario, Dynamic Programming (DP) method, numerically solves the problem to find global optimal behaviour [6]. This computationally highly demanding theoretical approach, does not promise a real-time implementation, however it gives very useful hints about the optimal behaviour of the complete system in entire trip which can also be approximated by heuristic algorithms [7]. Moreover, the optimality is a reference behaviour which can be exploited as a benchmark method to compare more practical methods [8]. Other approaches are also proposed based on numerical search algorithms like genetic algorithms [9]. Analytical optimization methods are also utilized where the optimization problem of HEV energy management is mapped to an optimal control problem and conventional optimal control techniques such as Pontyriagin Minimum Principle (PMP) are used [10]. Similarly in [11], a method that approximates the PMP is developed for real-time implementation purposes. Another analytical method based on "extremum seeking" is developed in [12] to optimize the energy management of a parallel hybrid and comparable results are achieved with respect to benchmark method based on DP.

On the other hand, real-time capable, less computationally demanding algorithms exist and already providing comparable results in simulation and real applications. Equivalent Consumption Minimization Strategy (ECMS) is one of them, which basically offers an equivalency factor between electrical (battery) and chemical (fuel) energy consumption characteristics [13]. Variants of this method proposes map based approaches to ease the implementation and fast computation [14].

On the other hand, ECMS necessitates an overwhelming calibration procedure in order to keep the battery state of charge (SOC) between high and low SOC band as well as sustaining the battery charge over the trip. Therefore, some studies enhanced the ECMS by using some additional SOC control factor in order to keep the SOC within the required battery operation ranges, with some additional cost due to the control effort which cause deviations from optimal behaviour. In [15] various SOC control approaches based on ECMS are compared.

Finally a recent focus point of active research topics is to utilize prediction based algorithms supported by various information sources such as GPS, digital map information or traffic flow data through advanced navigation systems [16]. This allows to optimize the energy flow not instantaneously but also over the route using future road and driving conditions.

A similar approach is applied in this paper to predictively control battery SOC, especially under real-world driving condition considering road topology and anticipation of recuperation zones along the route. Especially very long downhill route segments are offering high potential for recuperation by using e-braking via electrical motors in generator mode. While using state of the art methodology, such as ECMS that can only optimize the energy flow by using instantaneous information, this kind of free energy recovery zones cannot be fully exploited. Similarly upcoming uphill routes will cause an excessive torque demand for the engine, hence a higher fuel consumption if the battery charge is not prepared previously to drive this hill.

This paper demonstrates respectively the DP, ECMS and an extension to the ECMS approaches developed for a parallel HEV powertrain. The novel predictive ECMS method pre-emptively utilizes the road altitude information in energy management system to improve the overall recuperation and fuel consumption behaviour. The results are demonstrated using simulation models based on mathematical representation of vehicle and powertrain components as well as the road and speed conditions.

The rest of the paper is outlined as follows: Second chapter introduces the vehicle and powertrain model and key vehicle parameters used in the study. Third chapter explains respectively, DP, ECMS and ECMS with SOC control method. Four chapter is devoted to the novel predictive ECMS method and final chapter concludes the study with key simulation results.

2. POWERTRAIN AND VEHICLE MODEL FOR A PARALLEL HEV TOPOLOGY (PARALEL BIR HEA TOPOLOJİSİ İÇİN GÜÇ AKTARMA ORGANLARI VE ARAÇ MODELİ)

A quasi-static modelling approach is used to model the vehicle and powertrain behaviour. This approach is based on an assumption of a perfect speed tracking of the vehicle for a given drive-cycle. The traction forces and powertrain rotational speeds are calculated accordingly using the speed profile hence the electrical and fuel consumption via component efficiency behaviour models.

The vehicle, in most general road condition, is subjected to the resistance and inertial forces depicted in Figure 1. F_d, being the inertial force, F_a aerodynamic resistance force acting on the vehicle, F_r, rolling resistance force, F_g, force action due to road inclination and F_t, traction force are calculated by Eqs. (1-5).

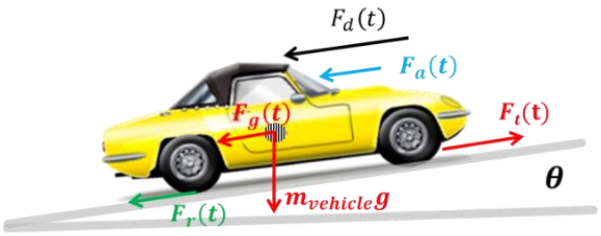

Figure 1: Generalized Force Equilibrium on the Vehicle (Araç Üzerindeki Genelleştirilmş Kuvvet Eşitliği)

$$F_d(t) = m_{vehicle}a(t) \quad (1)$$

$$F_a(t) = \frac{1}{2}\rho A_f C_d V^2(t) \quad (2)$$

$$F_g(t) = m_{vehicle}g\ sin\theta(t) \quad (3)$$

$$F_r(t) = m_{vehicle}gcos\theta(t)\eta_{roll.ress} \quad (4)$$

$$F_t(t) = F_d(t) + F_a(t) + F_r(t) + F_g(t) \quad (5)$$

Here $m_{vehicle}$ represents the vehicle mass, $a(t)$ longitudinal vehicle acceleration, ρ is the air density, A_f is front cross section area of the car, C_d is the aerodynamical resistance constant, θ is the inclination angle of the route, and $\eta_{roll.ress}$ is the tire rolling resistance factor.

A front wheel driven, parallel hybrid powertrain topology used in this study as depicted in Figure 2 with mechanical and electrical energy flows over the powertrain components. As seen in the figure, the stored electrical energy in the battery is used to power electric motors (EM). Based on the split factor, the mechanical energy of EM can be combined with Internal Combustion Engine (ICE) torque and propels the wheels over a 5-speed Automatic Transmission (AT) and differential. In case of zero torque of EM or ICE this topology allows both pure EM driving (ICE is off) or pure thermal mode (only ICE).

As seen in the figure, an additional mode allows to charge the battery during traction over EM which runs in generator (GEN) mode where ICE torque is split between wheel load and GEN torque to charge the battery.

One final operation mode available with this powertrain is the recuperative braking where EM is contributing the necessary braking torque to charge the battery, depending on the available maximum torque.

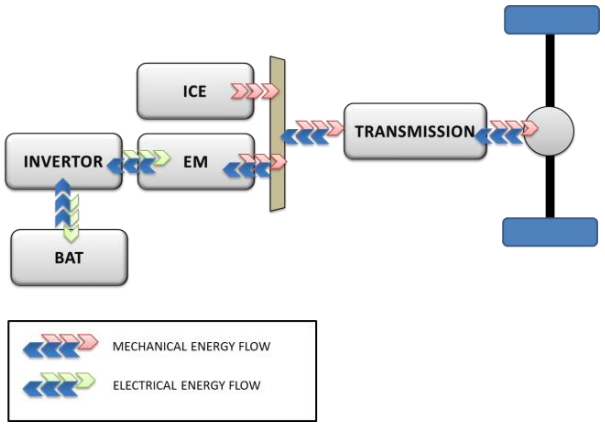

Figure 2: Parallel Hybrid Electric Vehicle Topology (Paralel Hibrit Elektrikli Araç Topolojisi)

A 25 kW permanent magnet brushless DC electric motor model together with a 75 kW diesel engine is modelled as a powertrain model. AT is a 5 speed automatic transmission and the torque converter behaviour is neglected in this study. Other key data about the simulated vehicle and powertrain are summarized in Table 1.

Table 1: Key Vehicle and Powertrain Parameters (Temel Araç ve Güç Aktarma Organları Parametreleri)

Parameter	Unit	Value
Max. Bat. Capacity	**Ah**	6.2
Nominal Bat. Voltage	**V**	310
Bat. Internal Resistance	**Ω**	2.5
Max. EM Torque	**Nm**	155
Max. EM Power	**kW**	25
Max. ICE Power	**kW**	75
Gear [-]	-	5 Speed AT
Vehicle Mass	**kg**	1600

To overcome the resistance force defined in Eq. (5), the net torque at wheel level can be found by:

$$T_{net@wheel}(t) = F_t(t)R_{eff} \quad (6)$$

while R_{eff} is the effective tire radius.

This $T_{net@wheel}(t)$, as explained above, is provided by $T_{ICE}(t)$and EM/GEN torque, $T_{EM}(t)$ split by a factor *u(t)*. Hence, *u(t)=1* implies pure thermal mode, whereas *u(t)=0* indicates pure electric mode.

$$T_{ICE}(t) = \frac{T_{net@wheel}(t).u(t)}{i_{tr}(N).i_{diff}.\eta_{tr}(N).\eta_{dif}} \quad (7)$$

$$T_{EM}(t) = \frac{T_{net@wheel}(t).(1-u(t))}{i_{tr}(N).i_{diff}.\eta_{tr}(N).\eta_{dif}} \quad (8)$$

The split factor *u(t)* is dynamically adjusted by the Energy Management system based on efficiency conditions of overall vehicle and powertrain systems as it will be explained in following section. It should be noted that the values of *u(t)>1* correspond to parallel charging mode where traction is only provided by engine power which is partly used to charge the battery over electric motor operating in GEN mode. Transmission efficiency, η_{tr} depending on the selected gear, N and being and differential efficiency η_{dif} are considered. ICE and EM efficiency behaviours depends on output torque and rotational speed. In Figure 3, the overall EM efficiency behaviour is mapped for EM speed and positive (traction) and negative (generator) torque.

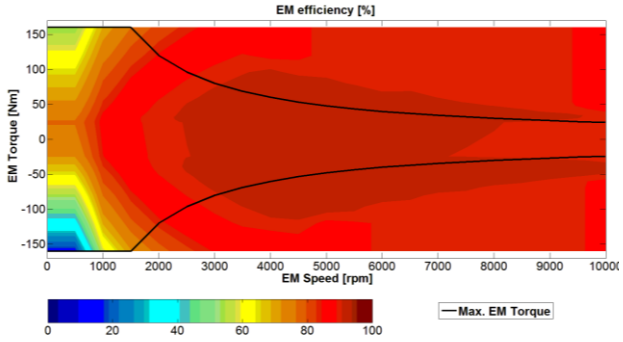

Figure 3: Electric Motor and Generator Efficiency and Maximum Torque Curve (Elektrik Motoru ve Jeneratör Verim ve Maksimum Tork Eğrisi)

As briefly mentioned above, ICE efficiency is similarly represented dependent on engine torque and speed, in other words, operating points of the engine. This behaviour that is statically mapped can be expressed by Eq. (9), where $\dot{m}_{fuel}$ depicts the fuel consumption per second and ω_{ICE} and T_{ICE} are engine speed and torque respectively.

$$\dot{m}_{fuel}(t) = f(\omega_{ICE}, T_{ICE}) \tag{9}$$

Battery behaviour is modelled by an equivalent circuit of an Open Circuit Voltage as depicted in Figure 4. With this model, the battery internal resistance, represented by R_i and U_{OC} are additionally functions of state of charge (SOC). The equivalent circuit, can be represented by Eq. (10) .

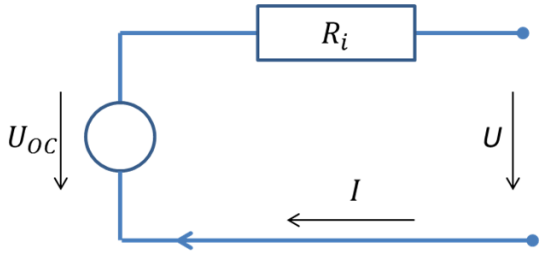

Figure 4: Open Circuit Voltage Circuit of HEV Battery System (HEA Batarya Sistemi Açık Gerilim Devresi)

$$I_{ch/dc}(t) = \frac{U_{oc}(t) - \sqrt{\left(\left(U_{OC}^2(t)\right) - 4P_{el.}(t) \cdot R_i\right)}}{2 \cdot R_i} \tag{10}$$

Being $P_{el}(t)$ battery power and $I_{ch/dc}$ is charging or discharging current depending on the sign of $P_{el}(t)$.
The unique dynamical of all model is used for SOC description

$$SOC(t) = -\frac{1}{Q_{max}} \int I_{ch/dc}(t)dt \tag{11}$$

where Q_{max} is maximum battery capacity. The battery equations do not imply any SOC limit for the useful energy content. However, it is always preferred to operate the battery within a certain SOC band (e.g. SOC_{low} = %40 and SOC_{high} = %60) for improved battery life. As it will be explained in next section, the battery SOC band will be considered inside the energy management system.

3. ENERGY MANAGEMENT STRATEGIES FOR PARALLEL HEV (PARALEL HEA İÇİN ENERJİ YÖNETİM STRATEJİLERİ)

As an optimization problem, a parallel HEV energy flow optimization is basically control the energy flow in most optimal way resulting with minimum fuel consumption. This implies the adjustment of energy flow from fuel tank or from/to battery being battery energy flow is bi-directional. This optimal adjustment, should not violate the main condition of providing the necessary traction or braking power to the wheels. In addition to that, operational constraints of powertrain and battery system should also be satisfied. These are mainly, physical constraints such as minim and maximum speed and torque of ICE and EM, as well as the maximum battery power, or SOC window consisting of SOC_{high} and SOC_{low}.

A cost function, $J(k)$ in discrete time domain is introduced representing the energy consumption of the fuel calculated by instantaneous consumption and Lower Heating Value Q_{LHV} of fuel:

$$J(k) = \sum_{k=0}^{N} \dot{m}_{ICE}(k).Q_{LHV} + \varphi_{SOC}(k) + \varphi_{SOC,f}(N) \tag{12}$$

Two additional terms are penalty functions to force the SOC remained in the defined SOC window and provide a charge sustaining behaviour at the end of the drive cycle:

$$\varphi_{SOC}(k) = \begin{cases} 0 & SOC(k) \in [SOC_{min.}, SOC_{max.}] \\ \infty & else \end{cases} \tag{13}$$

$$\varphi_{SOC,f}(k) = \begin{cases} 0 & SOC(N) = SOC_i \\ \infty & else \end{cases} \tag{14}$$

As explained above, a unique state of the system can be restructured in convenient form as follows:

$$\dot{SOC}(k) = -\frac{I(k)}{Q_{max}}\Delta t \tag{15}$$

defining the SOC change rate in dıscrete time domain.

Considering the operational and kinematic constraints of powertrain components as well as the battery operational range, following limits should not be violated as a result of the optimization:

$$\begin{aligned} & w_{ICEmin} \le w_{ICE}(k) \le w_{ICEmax} \\ & 0 \le w_{EM}(k) \le w_{EMmax} \\ & 0 \le T_{ICE}(k) \le T_{ICEmax}(w_{ICE}(k)) \\ & T_{EMmin}\big(w_{EM}(k)\big) \le T_{EM}(k) \le T_{EMmax}\big(w_{EM}(k)\big) \\ & P_{el}(k) \le P_{bat.max} \end{aligned} \tag{16}$$

Having all the kinematic, dynamic equations as well as the state and control constraints, the optimization problem is to be solved with an appropriate optimization methodologies. In other words, the optimization problem aims to calculate optimal *u(k)*, hybrid split factor for all instant of a driving mission specified by vehicle velocity and road inclination.

a. Global Optimal Behaviour Calculation With Dynamic Programming Method (Dinamik Programlama Metodu ile Global Optimal Davranış Hesabı)

To solve this non-linear dynamics characteristics of the vehicle-powertrain system, a well-known numerical optimization method, Dynamic Programming (DP) has been used. This method, relying on Bellman Principle of Optimality [17], guarantees globally the optimality of the problem, by solving discrete-time system starting from last time sequence and moving in backwards direction.

As seen in Figure 5, starting from final time, t = t_f, towards back to starting point t = *0* the cost function defined in Eq. (12) is calculated for each sampling time, k, at each discretized state value,

$$x_i \in [SOC_{min.}, SOC_{min.} + \delta SOC, \dots, SOC_{max.} - \delta SOC, SOC_{max.}]_{1XM}$$

and for each split value as defined in (7) and (8),

$$u_i \in [0, \delta u, \dots, u_{max.} - \delta u, u_{max.}]_{1XN}.$$

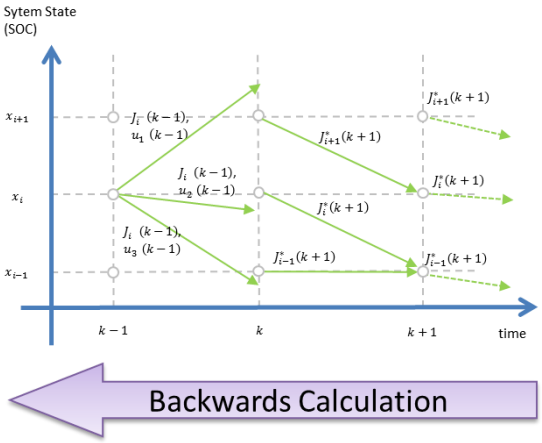

Figure 5: Backwards Calculation via DP With Cost Values Calculation at Each Time-Step (DP ile Ters Yönde Her Zaman Adımında Bedel Fonksiyonu Hesabı)

The minimum cost value, denoted by $J^*_i(k+1)$, for a specific time step k that brings the system state from $x_i(k)$ to any other state $x_{i+\varepsilon}(k+1)$ and the corresponding split factor $u^*_i(k+1)$ are stored as instantaneous minimum function. According to optimality principle, these optimal cost values and corresponding optimal split factors can be summed up with the cost values of the next time step (calculated in previous step). If for discrete input values u_i the new state at $x_{i+\varepsilon}(k+1)$ does not correspond to one of the pre-defined discrete values of x_i, a linear interpolation is applied to calculate the approximate cost values of exact state value.

Hence at any time, the minimum cost of going to the final time from any state $x_i(k)$ is available. Once the iteration is completed until *k=0*, the information of all optimal path at each discrete state until the very end of driving mission is available. A set of cost-values (and their optimal inputs) for each discrete state, x_i and discrete time, k are stored in a cost-to-go matrix. The matrix is then be re-used to calculate the optimal split values when the system is at any state values.

This backwards calculation is carried out for a given driving mission, specified by speed profile and road condition. Therefore the optimization method depends a priori information of road condition and speed profile. Furthermore, the iterative calculation routine and minimization process is computationally very intensive especially with reduced discretization factor and time-step to improve the accuracy. This causes also exponentially increasing storing capacity requirements. Therefore, DP method is considered as a benchmark optimization calculation by its globally optimizing characteristics and hence is used to compare other developed sub-optimal methodologies.

In Table 2 the overview of the hybrid modes which are available for the parallel hybrid vehicle topology is seen. In Figure 6, the selected operating modes as a

result of DP calculation and SOC profile over the drive-cycle NEDC can be seen. The road profile is assumed to be flat over the cycle. Figure 7 illustrates the $T_{ICE}(t)$, $T_{EM}(t)$ and selected gear.

Table 2: Operating Modes of Parallel Hybrid Electric Vehicle Topology (Paralel Hibrit Elektrikli Araç Topolojisi Çalışma Modları)

Operation Modes	Description
Mode 1	Split Mode
Mode 2	Parallel Charge
Mode 3	Recuperative Braking
Mode 4	Pure ICE
Mode 5	Pure EM
Mode 6	Standstill

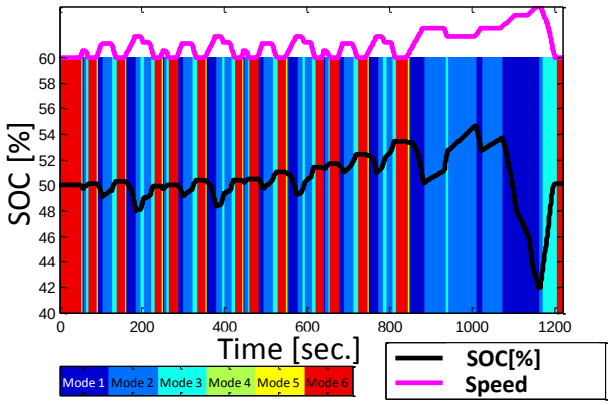

Figure 6: Vehicle Speed - Hybrid Operating Modes and SOC Over NEDC (NEDC Boyunca Araç Hızı, Hibrit Çalışma Modları ve Batarya Şarjı)

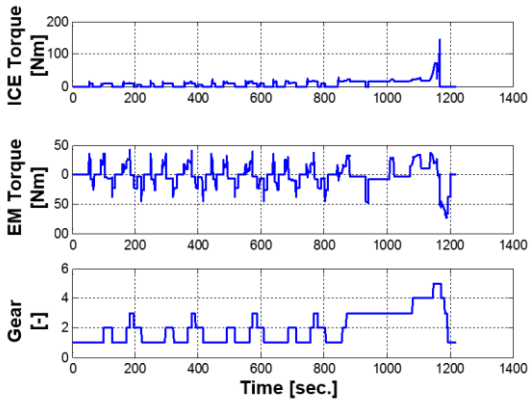

Figure 7: Engine Torque, EM torque and Selected Gear Over NEDC (NEDC Boyunca İYM Torku, EM Torku ve Seçili olan Vites)

b. Equivalent Consumption Minimization Strategy (Eşdeğer Yakıt Tüketimi Minimizasyonu Stratejisi)

Drawbacks of DP method in terms of computational effort and prior information of drive cycle and road information brings the necessity of developing a method based on instantaneous road and vehicle information. The Equivalent Consumption Minimization Strategy (ECMS) introduces an equivalence factor that balances the electrical energy consumption drawn from battery with respect to fuel consumption. In other words the total consumption of electrical energy and fuel energy can be combined in single parameter which is called equivalent fuel consumption computed by

$$\dot{m}_{equivalent} = \dot{m}_{ICE} + \dot{m}_{BAT,eq.} = \dot{m}_{ICE}(\omega_{ICE}(t), T_{ICE}(t), u(t)) + s_o.\frac{P_{el.}(u(t))}{Q_{LHV}} \quad (17)$$

Here, beside the real fuel consumption, $\dot{m}_{ICE}$, a virtual consumption value $\dot{m}_{BAT,eq.}$ is used. The latter represents the virtual fuel consumption which is equivalent to the stored energy in the battery by charging via ICE and recuperation and discharged energy by traction with EM. An equivalence factor s_o is used to convert this battery energy to its chemical energy equivalence (or equivalent consumed fuel with respect to stored or consumed battery energy, $\dot{m}_{BAT,eq.}$).

Before introducing the calculation method of equivalence factor s_o, a physical analogy is introduced to refer how $\dot{m}_{BAT,eq.}$ is obtained in two different modes of hybrid strategy. Firstly, for the split mode, the $\dot{m}_{BAT,eq.}$ represents the future consumed fuel amount that would be used to charge same amount of battery energy (see virtual charge and consumption in Figure 8). Similarly, for the parallel charge mode, the saved energy by charging the battery, has an equivalence of saved fuel that would be consumed if this charged energy was used for traction with engine (see virtual discharge and fuel saving in Figure 9).

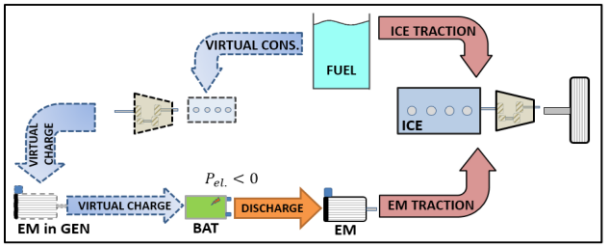

Figure 8: Physical Analogy of ECMS with Virtual Charging and Virtual Consumption in Split Mode (EYTM'nin Güç Ayrımı Modunda, Sanal Şarj ve Sanal Tüketiminin Fiziksel Analojisi)

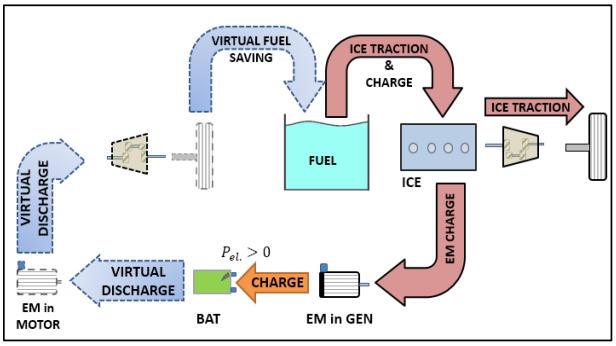

Figure 9: Physical Analogy of ECMS with Virtual Discharging and Virtual Consumption in Parallel Charging Mode (EYTM'nin Paralel Şarj Modunda, Sanal Deşarj ve Sanal Tüketiminin Fiziksel Analojisi)

A key part of the ECMS method is the representation of the equivalence factor, s_o which represents the ratio of average electrical and chemical energy consumption (or equivalent fuel consumption) for this specific powertrain for a given drive cycle. In other words, this parameter represents implicitly the mean efficiency of charging and discharging characteristics of the vehicle.

One important characteristics of the equivalence factor is its linearity for split and parallel charge modes for the entire drive cycle. As seen in Figure 10, over NEDC total fuel chemical energy and battery electrical energy are highly linear, for various constant split values u, whereas the linearity differs for parallel charging and split modes. Note that for $u=0$ there is still some negative energy stored in battery which corresponds to free recuperation energy over the drive cycle.

Depending on this two linear characteristics, equivalence factor can be defined separately for charging and discharging cases.

$$s_0 = \begin{cases} s_{0,charge} & P_{el.} > 0 \\ s_{0,discharge} & P_{el.} < 0 \end{cases} \quad (18)$$

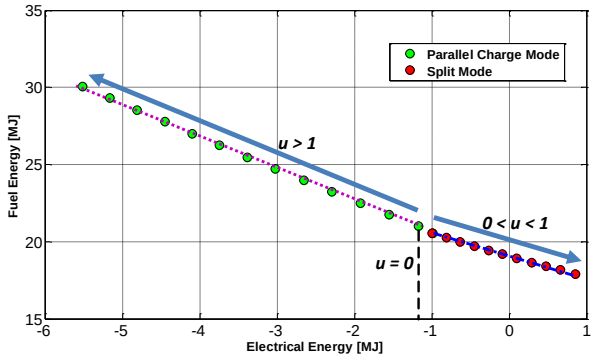

Figure 10: Linear Behaviour of Fuel Chemical Energy vs. Battery Electrical Energy for Various u Values (Yakıt Kimyasal Enerjisi vs. Batarya Elektrik Enerjisi'nin farklı u değerleri için Lineer Davranışı)

c. Comparison of DP and ECMS method (DP ve EYTM metodlarının karşılaştırılması)

The implementation of ECMS method is straightforward and computationally much less demanding compared to DP algorithm. Once the calibration of the equivalence factor is carried out, the equivalence consumption in Eq. (17) is calculated at each sampling time for all split values u. Hence, the equivalent consumption equation is acted like a cost function to be minimized instantaneously:

$$u = argmin\,(\dot{m}_{equivalent}) =$$
$$argmin\left\{\dot{m}_{ICE}(\omega_{ICE}(t), T_{ICE}(t), u(t)) + s_o.\frac{P_{el.}(u(t))}{Q_{LHV}}\right\} \quad (19)$$

Therefore, the real-time implementation consists of the minimization of one single equation calculated at each sampling time. Therefore ECMS application is viable in terms of real implementation. However, as stated above, the problem has been approached with average behaviour which makes the method is sub-optimal by definition.

The sub-optimality is highly dependent on the calibration of s_o factor which differs for each speed profile as well as road condition. However, once it is tuned for specific drive cycle the behaviour is closed to global optimal results. In Figure 11 to Figure 14, two different cycles, NEDC and FTP75 are simulated to compare the achieved behaviour of ECMS compared to DP.

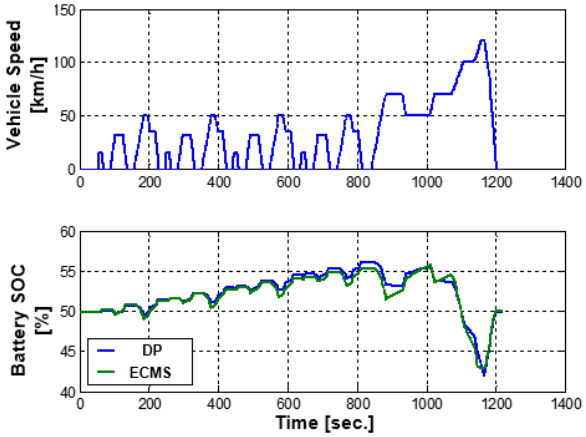

Figure 11: NEDC: Vehicle Speed and SOC Profile for DP and ECMS (NEDC: DP ve EYTM için Araç Hızı ve Batarya Şarj Profili)

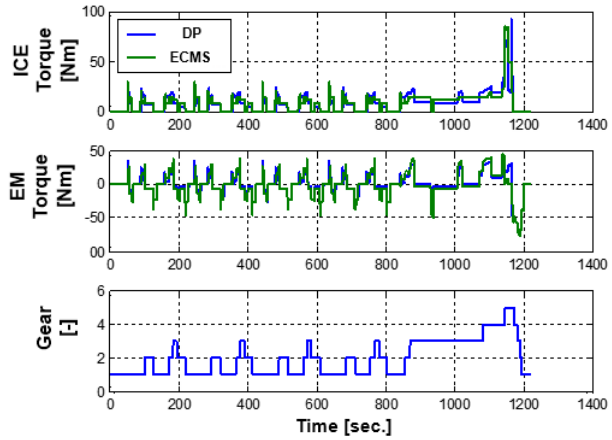

Figure 12: NEDC: T_{ICE}, T_{EM} , Selected Gear for DP and ECMS (NEDC: DP ve EYTM için İYM ve EM Torkları, Seçili Olan Vites)

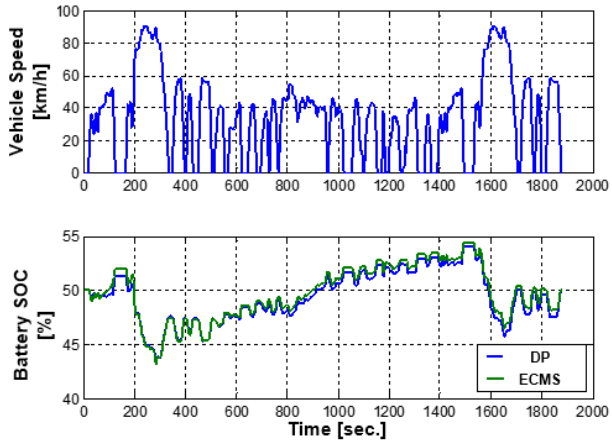

Figure 13: FTP Cycle: Speed and SOC Profile for DP and ECMS (FTP Çevrimi: DP ve EYTM için Araç Hızı ve Batarya Şarj Profili)

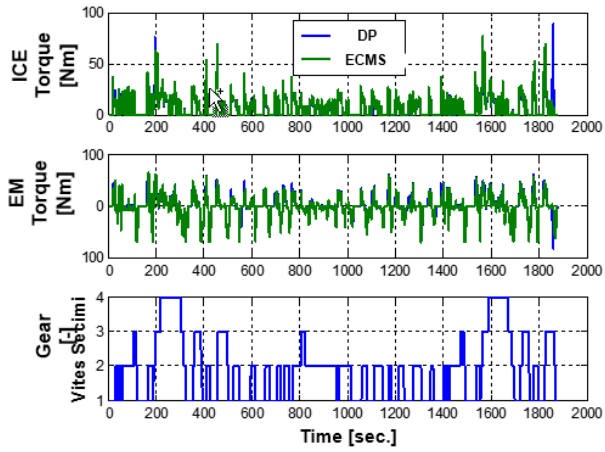

Figure 14: FTP Cycle: T_{ICE}, T_{EM} , Selected Gear for DP and ECMS (FTP Çevrimi: DP ve EYTM için İYM ve EM Torkları, Seçili Olan Vites)

As seen in SOC profiles as well as, TICE and TEM ECMS approaches the DP behaviour. Fuel Consumption values over these 2 cycles are summarized in Table 3 and Table **4**.

Table 3: Cumulative Fuel Consumption Obtained with DP and ECMS Over Different Drive Cycles (DP ve EYTM ile Farklı Sürüş Çevrimlerinde Elde Edilmiş Toplam Yakıt Tüketimleri)

Total Consumed Fuel [L]

	DP	**ECMS**
NEDC	520	524
FTP	761	766

Table 4: Average Fuel Consumption Obtained with DP and ECMS over Different Drivve Cycles (DP ve EYTM ile Farklı Sürüş Çevrimlerinde Elde Edilmiş Ortalama Yakıt Tüketimleri)

Average Fuel Consumption [L/100 km]

	DP	**ECMS**
NEDC	4.75	4.79
FTP	4.28	4.31

4. SOC BALANCE FACTOR FOR CHARGE SUSTAINING and ANTICIPATED ROAD GRADIENT (ŞARJ DENGELEME İÇİN ŞARJ DURUMU FAKTÖRÜ VE YOL EĞİMİ KESTİRİMİ)

Although ECMS provides good-match of optimality in terms of fuel consumption and ease of implementation with intensively reduced computational burden, a prerequisite of SOC balance between initial and end of cycle $SOC(t_0) = SOC(t_f)$ has to be guaranteed. This is essential in order to prevent excessive charge or discharge states at the end of cycle to be able to make a fair comparison. Eq. (19) misses such SOC balance factor. Therefore as stated in previous section such behaviour is provided by a well-calibration s_0 parameter which implies again a priori-known of speed profile. However this causes a problem for the real implementation where the implementation operates under unknown speed conditions. Therefore ECMS method is included a penalty function s_1 to guarantee the SOC balance between initial and terminal conditions:

$$\dot{m}_{equivalent} = \dot{m}_{ICE}\big(t, \omega(t), T_{ICE}(t), u(t)\big) + s_o . \frac{P_{el.}(t,u(t))}{Q_{LHV}} . s_1(\mathrm{SOC}) \quad (20)$$

where

$$s_1(SOC) = \begin{cases} \left(1 + \left(\frac{SOC_f - SOC(t)}{SOC_f - SOC_{min}}\right)^{2n+1}\right) & if\ SOC(t) < SOC_f \\ \left(1 - \left(\frac{SOC(t) - SOC_f}{SOC_{max} - SOC_f}\right)^{2m+1}\right) & if\ SOC(t) \geq SOC_f \end{cases} \quad (21)$$

Eq. (21) implies a multiplicative correction factor to original ECMS equation as in Eq. (21), where SOC_{min} and SOC_{max} are admissible battery SOC values, while n and m are integer numbers. The shape of the s_1 function motivates a more aggressive impact when the SOC approaches to the boundaries.

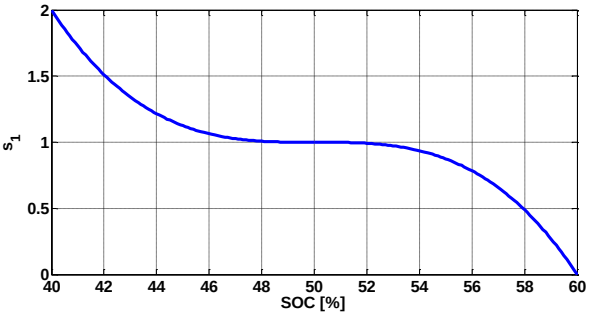

Figure 15: s_1 Penalty Function vs. *SOC* for SOC_{min} = *40%*, SOC_{max} = *60%*, SOC_f = *40%*, *n = 1* and *m = 1* (*SOC_{min} = 40%*, *SOC_{max} = 60%*, *SOC_f = 40%*, *n = 1* ve *m = 1* için s_1 Ceza Fonksiyonu vs. *SOC*)

Eq. (21) implies a multiplicative correction factor to original ECMS equation as in Eq. (21), where SOC_{min} and SOC_{max} are admissible battery SOC values, while n and m are integer numbers. The shape of s_1 function motivates a more aggressive impact when the SOC approaches to the SOC window boundaries.

On one hand, SOC balancing penalty function allows a charge sustaining behaviour over the cycle, on the other hand it increases the control effort over the complete ECMS equation that would deviate the optimal character. In this section, this additional stress is reduced by anticipating charging section over the route and utilizing this preparing the charge level against this free-charging recuperation energy. Then the method is further extended to deal with uphill road conditions by pre-charging strategy.

As seen in Figure 16, in most general case, in the absence of SOC control factor, s_1, a downhill route section followed by a flat road possesses a high recuperation energy potential. Since, by definition SOC will be limited by SOC_{max} level, some of the braking energy will be dissipated in friction brakes. To overcome this problem, a-priori knowledge of these potential recuperation zones, allows the pre-emptive control of SOC so that, a full recuperation can be achieved over the downhill section. Today's navigation systems permit the utilization of such road profile ahead by means of advanced digital map stored on-board in a structured format called e-horizon. Furthermore, an accurate prediction of the speed profile is assumed to be obtained over the same route horizon with statistical and online traffic data as well as the traffic sign information of the route.

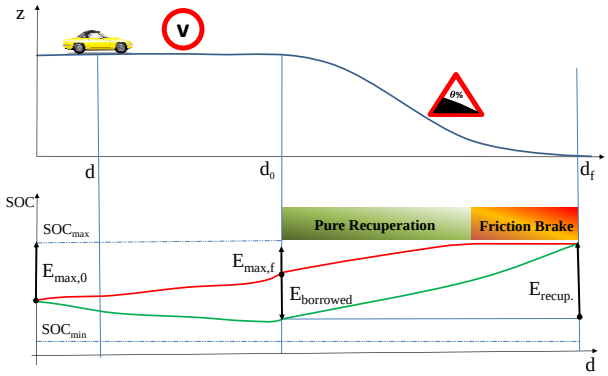

Figure 16: Top: Downhill Section Starting at d_o Bottom: SOC Profile for Non-predictive (red) and Predictive (green) on Downhill Section (Üst: d_o'dan Başlayan Aşağı Yönde Yokuş, Alt: Aşağı Yönde Yokuş Sırasında Öngörüsüz (kırmızı) ve Öngörülü (yeşil) Batarya Şarj Profili)

By still using the standard form of ECMS, SOC profile preparation to upcoming downhill section is possible by allowing ECMS to use or borrow some part of upcoming free recuperation energy in advance. For instance, the case depicted in Figure 16, for non-predictive ECMS, on the flat road section, SOC tends to increase by a result of parallel charging which is obviously a result of the instantaneous minimization of ECMS equation under these operational conditions. An additional term is implemented on the ECMS equation to change its characteristics such that ECMS function motivates more electric drive (e.g. split mode). Mathematically expressing the original ECMS Eq.(17) is modified by an additional term $\dot{m}_{recup.}$ as follows:

$$\dot{m}_{equivalent} = \dot{m}_{ICE} + \dot{m}_{BAT,eq.} + \dot{m}_{recup.} = \dot{m}_{ICE} + s_o.\left(\frac{P_{el.}(u(t))}{Q_{LHV}} + \frac{P_{borrowed}}{Q_{LHV}}\right) \quad (22)$$

$\dot{m}_{recup.}$ represents the equivalent fuel consumption of the borrowed recuperation energy. As seen again in Figure 16, this energy is calculated by remaining energy to fully charge the battery, $E_{max,0}$, remaining energy to fully charge the battery at the start of downhill (d_0), $E_{max,f}$ and total recuperation energy, E_{recup}. Recuperation energy can be calculated with vehicle longitudinal dynamics and estimated vehicle speed over the route section as in Eqs (1-5).

$$E_{recup.} = E_{road}.\lambda_{recup.} = F_t(\bar{V},\theta)\cdot\left(d_f - d_0\right).\lambda_{recup.} \quad (23)$$

$\lambda_{recup.}$ represents the average recuperation efficiency of the generator and all driveline while the brake energy is stored in battery. As depicted in Figure 16, borrowed energy to be drawn from battery is found by:

$$E_{borrowed} = E_{recup.} - E_{max,f} \quad (24)$$

where $E_{max,f}$ is estimated by the following linear equation:

$$E_{max,f}(t) = \kappa\left(SOC_{max} - SOC(t)\right) + E_{max,0} \quad (25)$$

This calculated borrowed energy constitutes of total energy that has to be drawn from battery until vehicle reaches d_0. Therefore Eq. (25) is calculated continuously at each instant while the vehicle approaches to start of downhill and hence the $\dot{m}_{recup.}$ In other words, equivalent fuel consumption of the borrowed energy corresponding to each covered distance is calculated and implemented in Eq. (22) by using:

$$\dot{m}_{recup.} = s_o.\frac{P_{borrowed}}{Q_{LHV}} = s_o.\frac{E_{borrowed}}{Q_{LHV}\cdot(d_0-d)} \quad (26)$$

A similar approach is applied for the upcoming uphill sections of the road to pre-charge the battery in order to use more battery energy for higher load sections of the route. As seen in Figure 16, the pre-charge energy is used during uphill where non-predictive control uses engine power for both charging the battery and propelling the vehicle to sustain the charge. This borrowed pre-charged energy taken from fuel is equivalent to:

$$E_{borrowed} = E_{uphill} - E_{min,f} \quad (27)$$

where E_{uphill} is the best-case battery energy necessary to drive the uphill electrically and $E_{min,f}$ is the energy that would be remained if non-predictive strategy is used. This borrowed energy is similarly put in first equation (26) and then (22) to store the necessary energy to drive the uphill more electrically.

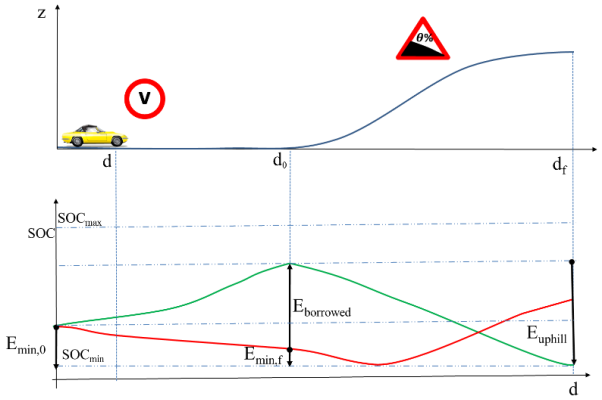

Figure 17: Top: Uphill Section Starting at d_0 Bottom: SOC Profile for Non-predictive (red) and Predictive (green) on Uphill Section (Üst: d_o'dan Başlayan Yukarı Yönde Yokuş, Alt: Yukarı Yönde Yokuş Sırasında Öngörüsüz (kırmızı) ve Öngörülü (yeşil) Batarya Şarj Profili)

The performance of this enhanced predictive ECMS is tested under similar scenarios illustrated in Figure 16 and Figure 17. Firstly a pure downhill scenario is presented with two different constant speed cases where the predictive ECMS is tested for both parallel charge and power split modes. Then a second scenario is created for a mixed road profile with uphill, downhill and flat sections. All road sections and their key parameters are summarized in Table 5.

Table 5: Road Sections and Speed Properties Used in Simulations (Simülasyonlarda Kullanılan Yol Bölümler ve Hız Profilleri)

		Route Sections				
Scenario	**Properties**	**Sec.1**	**Sec.2**	**Sec.3**	**Sec.4**	**Sec.5**
Scenario 1 Case 1	**Speed [km/h]**	50	50	-	-	-
	Length [km]	3	1.5	-	-	-
	Incl. [%]	0	-5	-	-	-
Scenario 1 Case 2	**Speed [km/h]**	60	50	-	-	-
	Length [km]	3	1.5	-	-	-
	Incl. [%]	0	-5	-	-	-
Scenario 2	**Speed [km/h]**	50	60	60	60	50
	Length [km]	1	1.5	6.5	3.8	2.8
	Incl. [%]	0	5	0	-5	0

The first Scenario starts at the point where the upcoming downhill section is anticipated which corresponds also to the moment where standard ECMS is abandoned (Eq. 17) and predictive ECMS (Eq. 22) is triggered.

Scenario 1 is varied for two different initial conditions where at the beginning of the scenario ECMS is operating the powertrain in split mode (Case 1) and parallel charge mode (Case 2). It is obvious that the predictive ECMS gain would be higher for the case where SOC tends to increase in Case 2 since the SOC would reach max charge limit earlier although predictive ECMS does at the end of the scenario. Vehicle speed is assumed to be 50 km/h in Case 1 and 60 km/h in Case 2.

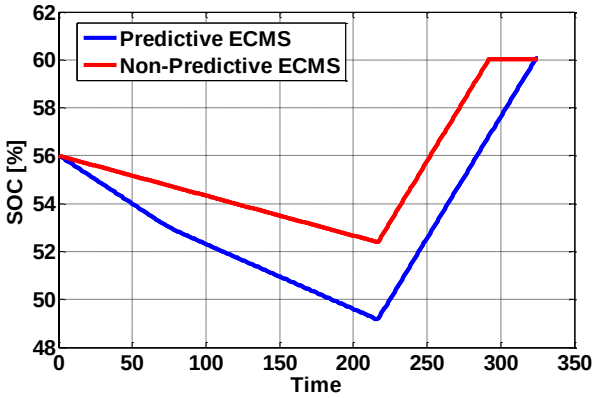

Figure 18: Case 1: *SOC(t_o)* = 0.56, *V = 50 km/h*, SOC vs. Time (Durum 1: *SOC(t_o)* = 0.56, *V = 50 km/sa*, SOC vs. Zaman)

As seen in Figure 18, non-predictive ECMS under instantaneous driving conditions operates the powertrain in split mode which is the (sub)-optimal condition. However, this behaviour causes a deficiency of recuperation energy by the end of the downhill section. Whereas this drawback is prevented by pre-discharge

with higher EM contribution to the drive torque and less engine torque. This pre-emptive SOC control allows to fully charge again the battery by the end of the downhill section.

In Case 2, as seen in Figure 19, same route is covered this time with higher speed. This motivates the parallel charge mode for the non-predictive ECMS again only due to the instantaneous condition which are independent from future road conditions. However, predictive ECMS, due to its predictive behaviour pre-discharge the battery similar to Case 1. Please note the difference in SOC profile of predictive ECMS in both cases which are the consequence of different road condition and efficiency behaviour of the powertrain for different vehicle speed.

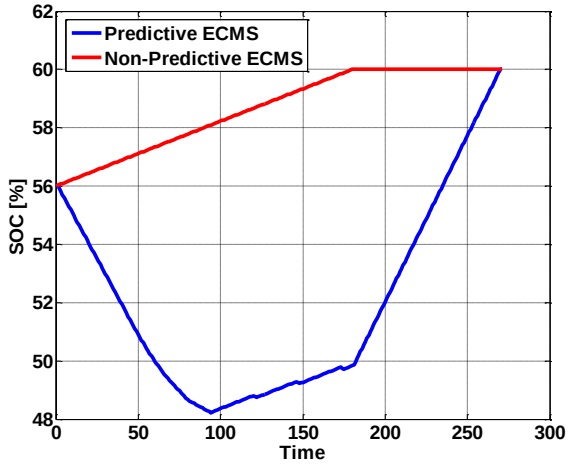

Figure 19: Case 2: $SOC(t_o)$ = 0.56, *V = 60 km/h*, SOC vs. Time (Durum 2: $SOC(t_o)$ = 0.56, *V = 60 km/sa*, SOC vs. Zaman)

The Scenario 2 includes as previously discussed both uphill and downhill road and also different speed values. The scenario starts with an upcoming uphill section where the non-predictive classical ECMS operates in split mode and hence the SOC level decreases in mainly in Section 1. As SOC balance is required, as soon as the battery is depleted, hybrid strategy switches to charging mode where the SOC starts to increase. When this charging load is combined with relatively high road load at uphill section, non-predictive ECMS starts to consume more fuel. However this is compensated via predictive ECMS, since the pre-charge allows to get over the uphill section with more electric power which consequently results with fuel consumption improvement. This phenomenon can be observed in Figure 20 in Section 1 and 2 as well as in fuel consumption values in Figure 21. The excessive consumption at Section 1 and 2 is due to the surplus torque for pre-charge which is then compensated at the rest of the manoeuver.

Second part of the Scenario 2 is similar to Scenario 1/Case 2 where the long downhill section is anticipated earlier therefore a pre-discharge mode is triggered that allows to fully discharge the battery which will be charged during the downhill section while the non-predictive ECMS algorithm will not be fully exploit the recuperation energy due to early filled battery capacity. Scenario 2 concludes with last flat road section (Section 5) where the SOC values of predictive and non-predictive ECMS algorithms are equal. This allows to make a fair comparison of fuel consumption of both cases since the fuel would not be used to charge one of the cases for a higher SOC level.

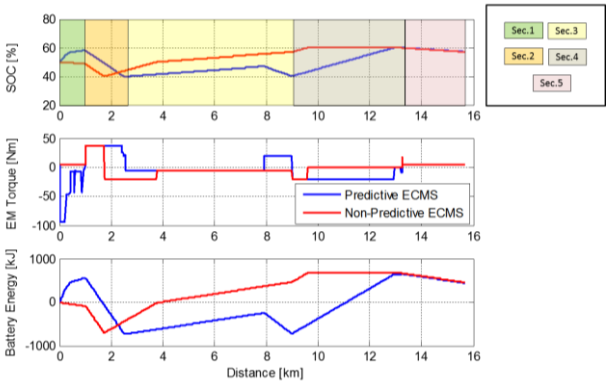

Figure 20: Scenario 2: Road Sections, SOC, EM Torque and Battery Energy (Senaryo 2: Yol Bölümleri, SOC, EM Torku ve Batarya Enerjisi)

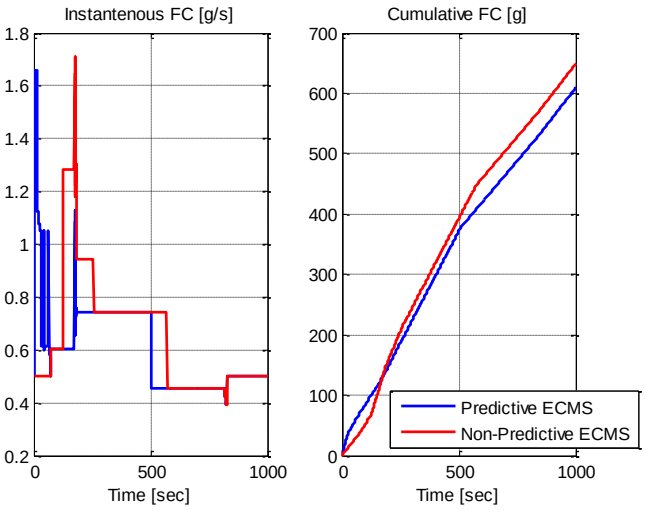

Figure 21: Scenario 2: Instantaneous and Cumulative Fuel Consumption (Senaryo 2: Anlık ve Toplam Yakıt Tüketimleri)

Improvements achieved by the predictive ECMS approach for the specified scenarios are summarized in

Table **6**. As cited above, Case 2 has higher improvements consumption value due to early charge saturation of non-predictive ECMS.

In Scenario 2 a combined improvement of 6% is obtained over a long route model including the uphill and downhill sections.

Table 6: Fuel Consumption Improvements with Predictive ECMS (Öngörülü EYTM ile Yakıt Tüketimi Tasarrufları)

SCENARIOS	FC Non-Predictive ECMS [g]	FC Predictive ECMS [g]	Improvement [%]
Scenario 1 Case 1	150.8	143.8	4.6%
Scenario 1 Case 2	175	151.1	13.7%
Scenario 2	648	609	6.0%

5. CONCLUSION (SONUÇ)

This study summarizes the development of a predictive energy management strategy for a parallel hybrid powertrain of a mid-sized passenger car. Firstly a theoretical optimization methodology based on Dynamic Programming (DP) is introduced to achieve the theoretical optimal limits of the studied vehicle and powertrain. Although the approach allows investigating the global optimal behaviour, it lacks the real-time capability due to its highly overwhelming computational burden. Therefore an alternative sub-optimal method called Equivalent Consumption Minimization Strategy (ECMS) is studied and benchmarked to DP. This computationally less complex and real-time feasible alternative is tested under various driving conditions which results comparable sub-optimal behaviour with respect to global optimum. However its lack of predictive nature prevents this ECMS approach to fully benefit from long recuperation condition because of downhill and uphill road conditions. This drawback is overcome thanks to newly developed predictive ECMS approach based on anticipation of uphill and downhill road conditions and modify the classical ECMS to either by pre-charging the batter or fully recuperate free braking energy.

6. REFERENCES (KAYNAKLAR)

1. "Creating the Clean Energy - Economy Analysis of the Electric Vehicle Industry", Technical Report, ***International Economic Development Council***, Washington, DC, (2013)
2. "Studying the PEV Market in California: Comparing the PEV, PHEV and Hybrid Markets", Technical Report, Gil Tal, Michael A. Nicholas, ***EVS27***, Barcelona, Spain, (2013)
3. "Hybrid Electric Vehicles - An overview of current technology and its application in developing and transitional countries", ***UNEP***, Kenya, (2009)
4. Serrao, L., Simona, O., Rizzoni. "A Comparative Analysis of Energy Management Strategies for Hybrid Electric Vehicles", ***Journal of Dynamic Systems***, Measurement, and Control, Vol. 133, (2011)
5. Salmasi, F., "Control Strategies for Hybrid Electric Vehicles: Evolution, Classification, Comparison, and Future Trends," ***IEEE Trans. Veh. Technol.***, 56(5), pp. 2393–2404, (2007)
6. Brahma, A., Guezennec, Y., and Rizzoni, G., "Optimal Energy Management in Series Hybrid Electric Vehicles," ***Proceedings of the 2000 American Control Conference***, Vol. 1, pp. 60–64, (2000)
7. Lin, C.-C., Peng, H., Grizzle, J. W., Liu, J., Busdiecker, M., "Control System Development for an Advanced-Technology Medium-Duty Hybrid Electric Truck." ***SAE***, (2003)
8. Schori, M., Boehme, T. J., Frank, B., Schultalbers, M., "Calibration of Parallel Hybrid Vehicles Based on Hybrid Optimal Control Theory", ***9th IFAC Symposium on Nonlinear Control Systems Toulouse***, France, September 4-6, (2013)
9. Zhao, Z., Hu, F., "Optimization of Control Parameters in Parallel Hybrid Electric Vehicles Using a Hybrid Genetic Algorithm", ***IEEE Vehicle Power and Propulsion Conference*** (VPPC), (2010)
10. Kim, N., Cha, S., Peng, H., "Optimal Control of Hybrid Electric Vehicles Based on Pontryagin's Minimum Principle", ***IEEE Transactions on Control Systems Technology***, (2010)
11. Cong, H., Ouyang, M. Xu, L., Wang, H. "Approximate Pontryagin's minimum principle applied to the energy management of plug-in hybrid electric vehicles", ***Applied Energy Journal***, Elsevier (2014)
12. Dincmen, E., Guvenc, B. A., "A Control Strategy for Parallel Hybrid Electric Vehicles Based On Extremum Seeking", ***Vehicle System Dynamics***, vol. 50, no. 2, pp. 199-227, (2012)
13. Musardo, C., Rizzoni, G., Staccia, B., "A-ECMS: An Adaptive Algorithm for Hybrid Electric Vehicle Energy Management", ***44th IEEE Conference on Decision and Control, and the European Control Conference***, Spain, (2005)
14. Sivertsson, M., Sundström, C., Eriksson, L., "Adaptive Control of a Hybrid Powertrain with Map-Based ECMS" ***World Congress***, Volume # 18 - Part 1, (2011)
15. Simona, O. Serrao, L., "On Adaptive-ECMS strategies for hybrid electric vehicles", ***Int. Scient. Conf. on hybrid and electric vehicles***, (2011)
16. Gong, Q., Tulpule, P., Marano, V., Midlam-Mohler, S., Rizzoni. G. "The Role of ITS in PHEV Performance Improvement", ***IEEE American Control Conference***, (2011)
17. Donald E. Kirk, "Optimal Control Theory: An Introduction", ***Dover Publications***, April 30, (2004)